

## Natural Gas Condensate Desulfurization via Polyacrylonitrile/Ag Nanocomposite Nanofibers: Optimization and Kinetics/isotherms Studies

R. Dadashvand-nigjeh<sup>1</sup>, A. Mollahosseini<sup>2\*</sup>, M. Alimoradi<sup>1</sup>,  
M. Ramezani<sup>1</sup>

<sup>1</sup> Department of Chemistry, Faculty of Science, Islamic Azad University, Arak, Islamic Republic of Iran

<sup>2</sup> Research Laboratory of Spectroscopy & Micro and Nano Extraction, Department of Chemistry, Iran University of Science and Technology, Tehran, Islamic Republic of Iran

Received: 16 June 2020 / Revised: 27 September 2020 / Accepted: 24 October 2020

### Abstract

In the present study for the first time, a novel polyacrylonitrile-silver nanocomposite nanofiber was synthesized by electrospinning for adsorbing sulfur compounds in natural gas condensate. The synthesized material was characterized by SEM, EDAX, and XRD. The presence of C, N, O, and Ag proved that the composite was synthesized successfully. In order to achieve the best adsorption conditions, the effect of contact time, adsorbent dosage and initial sulfur compound concentration was examined. Under optimal values, efficiency of greater than 90% was found. In addition, different isotherms and kinetics models were tested to describe the sorption process. It was found that Freundlich (0.9900) was superior to Langmuir (0.9688), Temkin (0.9648) and Dubinin-Radushkevich (0.8273) models, revealing that sulfur compounds tend to form multilayers on the heterogeneous surface of polyacrylonitrile-silver nanocomposite nanofiber. The energy value of the adsorption was 23.57 kJ/mol, indicating chemisorption reactions. Based on kinetics studies, the desulfurization by nanofibers followed Pseudo-second-order and Elovich kinetics. Finally, the desulfurization function of nanocomposite was studied and validated using adsorbent columns. The obtained results demonstrate polyacrylonitrile-silver nanocomposite nanofiber as a promising material in the field of desulfurization.

**Keywords:** Adsorption; Nanofiber; Natural gas condensate; Sulfur compounds.

### Introduction

Gas condensate is considered as one of the most valuable products derived from natural gas reservoirs, the price of which is slightly higher than those in crude oil on global markets. Cuts 5 and 6 are the major

components of gas condensate [1]. In addition, sulfur compounds are one of the most important contaminants of gas condensate which release toxic gases by combustion, damage metals, catalysts in the engine, and fuel cells [2, 3]. In this regard, the existing general methods for removing sulfur compounds of fuels

\* Corresponding author; Tel: +982173228342; Fax: +982173021578; Email: amollahosseini@iust.ac.ir

include: oxidation methods, adsorption via a solvent, surface absorption in stationary phase bed and hydrodesulphurization [4]. However, there are some disadvantages for the above-mentioned methods: such as the requirement for difficult operating conditions such as high temperature and high pressure; the necessity for expensive catalysts; high energy consumption and failure to remove some sulfur compounds. Therefore, providing a new, low-cost, and practical method is needed to remove these compounds from gas condensate to enhance its quality.

Traditional materials for adsorptive removal of sulfur are zeolites, activated carbon, and alumina, which are regarded as porous materials and perform desulfurization mainly via adsorption. The implementation of transition metal ions incorporated in these materials leads to reactive adsorption via  $\sigma$ - $\pi$  bonding between metal ions and adsorbates, which results in enhancing their performance [5]. Bakhtiari et al. [6] reported the optimization of sulfur adsorption over Ag-zeolite nano-adsorbent with a thiophene adsorption efficiency close to 50 ppm for 5.53% metal content. Another study, the combination of electrochemical oxidation and solvent extraction approaches was suggested to reduce the sulfur content in condensate gasoline down to 13.1  $\mu\text{g/g}$  with a desulfurization efficiency of 99.62% [7]. Furthermore, Adedibu et al. [8] synthesized zig-zag 1D coordination polymer of copper(II)  $[\text{Cu}(4\text{-mba})_2(\text{H}_2\text{O})_3]$  and revealed that this complex had the potential for desulfurization of fuel with an observed adsorption capacity of 9.6 mg/g at 32 °C for 6 h. More recently, the polystyrene nanofibrous membrane loaded by  $\text{Ag}^+$  cations can be employed for deep desulfurization [9]. Further, the desulfurization of gasoline was conducted by acrylonitrile electrospun nanofibers, including lead nanoparticles [10].

Nanocomposites and nanofibers are among the candidates which are used for filtration and purification as well as composites strengthening, fuel cells, electronic and tissue engineering [10-12]. The high surface-to-volume ratio, high flexibility in functionalizing of surfaces, and excellent mechanical properties are considered as some of the important features related to nanofiber composites compared to conventional fibers. Chemical vapor deposition, hydrothermal technique, mechano-chemical methods and electrospinning are of the primary composite preparation methods, that among them electrospinning has gained attention of many scholars [13-15]. Electrospinning is regarded as a simple and cost-effective approach for the synthesis of nanofibers [16, 17]. In the recent years, many researchers have tried to

synthesize fibrous composite for the removal/adsorption of nickel [18], chromate [19], methylene blue [20], congo red [15], methyl orange [21], protein [22], and mercury [23]. In view of sulfur compound removal, few number of studies have carried out. Desulfurization of gasoline using acrylonitrile electrospun nanofibers and lead nanoparticles led to removal efficiency and adsorption capacity of 93.31% and 31.4 mg S/g, respectively [10].

Utilization of noble metals with nanomaterials, including Pt, Ag and Au could improve the capacity of the composite, and many scholars suggested them as a promising material in the field of environmental technology and remediation. ZnO/Ag/GO nanocomposite was employed for the removal of naphthalene, and resulted in 92% degradation of the pollutant [24]. Yang et al. [25] proposed ZnO/Ag nanocomposites for dye elimination. Ammonia adsorption in Ag/AgI-coated hollow waveguide was also reported by Jinyi et al. [26]. Another nanocomposite namely, biogenic Ag@Fe was utilized for methyl red removal and resulted in maximum adsorption capacity of 125 mg/g [27]. In the case of gases, dimethylsulfide and t-butylmercaptan removal from pipeline natural gas fuel by means of Ag-zeolite was studied [28]. Nair and J. Tatarchuk (2011) attempted to remove species from hydrocarbon fuels by supported silver adsorbents [29]. Desulfurization of hydrocarbon fuels was also conducted by Ag/TiO<sub>2</sub> [30]. These reports are a clear demonstration of the fact that Ag could have superior adsorption capacity in the adsorption process to remove the contaminant such as sulfur species.

In the current study for the first time, electrospun polyacrylonitrile-silver nanocomposite was synthesized and utilized for desulfurizing condensate. The prepared nanocomposite was characterized, and then employed to investigate the effect of time and adsorbent dosage. The whole process was studied by kinetics and isotherm models.

## Materials and Methods

### Materials

The PAN powder, DMF, AgNO<sub>3</sub> and all other chemicals were all purchased from Sigma Aldrich (with high purity) and were used without further purification. Distilled water was used during the study.

### Characterization

First, a scanning electron microscope (FE-SEM; LEO 440i) was used to evaluate the morphology and surface structure of the synthesized nanocomposite. Then, the

XRD pattern of synthesized nanomaterial in this research was provided by the Siemens D5000 diffractometer. The concentration of remaining sulfur in the sample was measured using a total sulfur analyzer (TS3000, Thermo).

### Synthesis of nanocomposite

In order to prepare 11% w/w solution of PAN, the appropriate amount of polyacrylonitrile (PAN, MW = 80000) powder was weighed and added to DMF solvent and stirred for 2 hours by using a stirrer at ambient temperature. Then, the required amount of AgNO<sub>3</sub> powder was added to this solution and stirred for 24 hours by using a magnetic stirrer to prepare 45% w/w AgNO<sub>3</sub> solution toward the total weight of PAN and DMF.

For electrospinning, the prepared solution was drawn into a syringe with a stainless steel needle with 1 mm diameter attached to. The syringe was pushed by syringe pump (KDS 200, KD Scientific Inc., MA), and the needle tip was connected to a high voltage power supply (ES30P, Gamma High Voltage, FL) and aluminum sheet (20×20 cm) was used as the collector. The infusion rate, applied voltage, and distance of the needle to collector were 1.5 ml/h, 15 KV, and 15 cm, respectively.

### Measuring the sample adsorption capacity

In order to obtain the adsorption capacities of synthesized nanocomposites, they were poured into 5 mL of gas condensate with a primary sulfur concentration of 100 ppm and the amount of residual sulfur in the sample was measured using a total sulfur analyzer after stirring for 10 min. Finally, the capacity of adsorption was calculated by using the following equation (1):

$$q_e = \frac{(C_0 - C) * V}{m} \quad (1)$$

where  $q_e$  represents the adsorption capacity of synthesized nanofibers in mg of sulfur per gram of adsorbent,  $C_0$  and  $C$  are the initial and final concentration of sulfur in the sample in mg/L respectively, and  $V$  indicates the sample volume in liters, and  $m$  is regarded as the mass of the adsorbent in grams.

### Studies related to adsorption isotherms

In an Erlenmeyer flask, the amount of 30 mL of gas condensate containing 400 mg/L total sulfur was poured. Then, different amounts of nanocomposite were placed inside the flask, the mixture was stirred for 30 minutes, and the amount of total sulfur was measured. Then, the equilibrium adsorption capacity ( $q_e$ ) was

calculated from equation (2):

$$q_e = \frac{(C_0 - C_e) * V}{W} \quad (2)$$

In this equation,  $C_0$  indicates the initial concentration (mg/L),  $C_e$  is considered as the equilibrium concentration of sulfur compounds after 30 minutes (mg/L),  $V$  represents the volume of solution in liters, and  $W$  is the mass of the adsorbent in grams.

### Kinetic studies

In each two separate Erlenmeyer flasks, 10 mL of gas condensate including 150 and 400 mg/L total sulfur was poured. Then, 0.02 g of the nanocomposite was placed inside each of the flasks, the mixture was stirred, the amount of sulfur was measured at different time intervals and the adsorption capacity at different times was calculated from the equation (2).

## Results and Discussion

### Characterization

SEM images were used to observe the surface morphology of the synthesized material. Figure 1 shows the SEM image of polyacrylonitrile /Ag nanocomposite. As shown, the synthesized fibers are in the form of straight strips with a fairly uniform distribution. It demonstrates that the fibrous structure was prepared successfully due to its uniform structure. Figure 2 shows the EDAX analysis of electrospun polyacrylonitrile/Ag nanocomposite. Accordingly, the elements C, N, O, and Ag were detected in the synthesized nanocomposite, revealing that polyacrylonitrile and Ag are both present in the prepared material. In addition, the XRD pattern of the synthesized nanocomposite is shown in Figure 3. The characteristic peak of the polyacrylonitrile

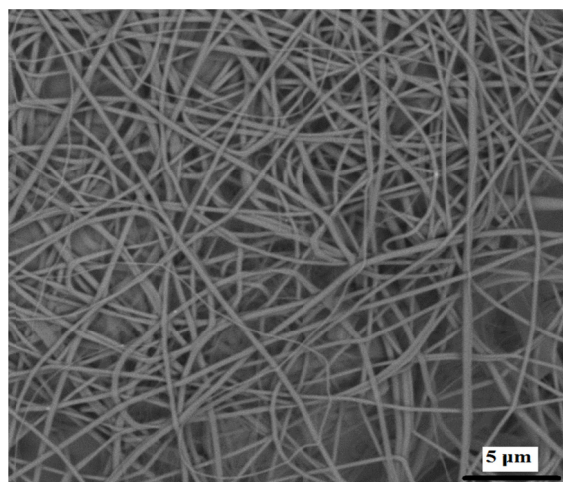


**Figure 1.** SEM images of polyacrylonitrile-silver nanocomposite nanofiber.

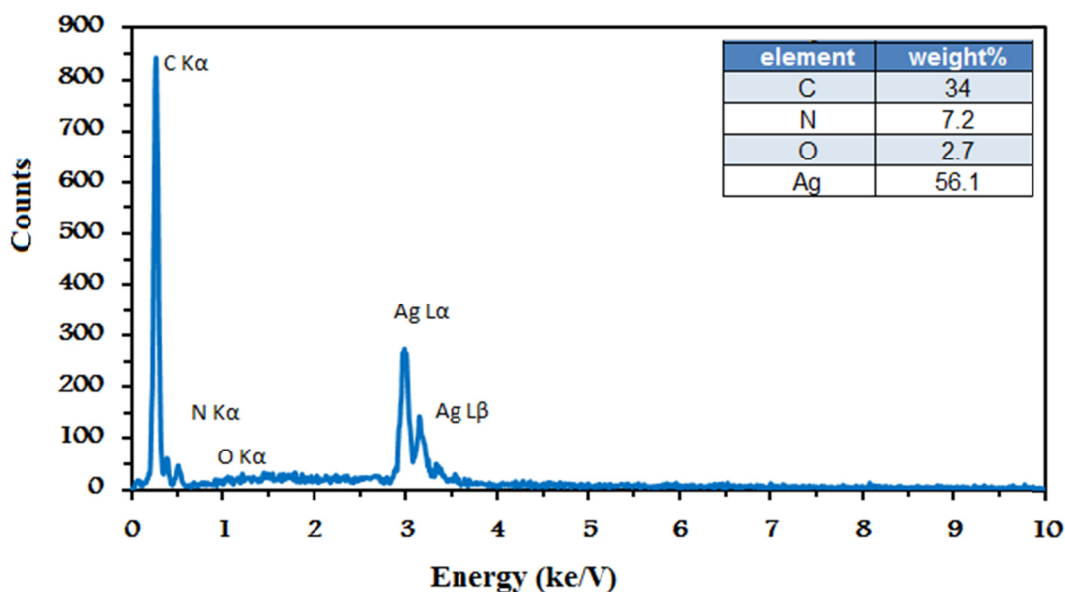


Figure 2. EDAX analysis for electrospun polyacrylonitrile /Ag nanocomposite.

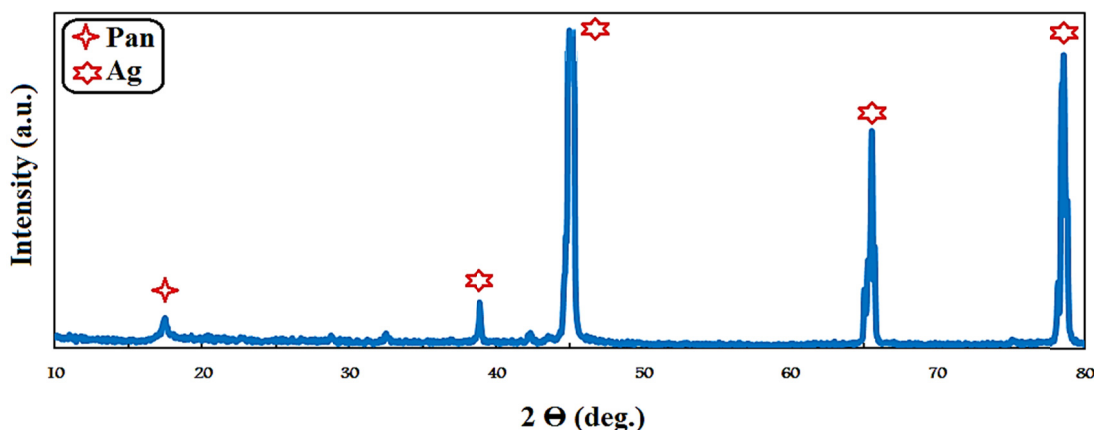


Figure 3. XRD analysis for electrospun polyacrylonitrile /Ag nanocomposite.

crystalline structure is located at  $2\theta$  of 17. The peaks related to silver phase including (111), (200), (220), and (311) are located at  $2\theta$ 's of 38, 45, 65.5, and 78.5, respectively, which confirms the presence of two phases in the nanocomposite. These characterizations are clearly indicative of the fact that polyacrylonitrile and Ag were both presented in the material, and also the nanocomposite has a fibrous structure which is beneficial in desulfurization process.

#### Optimization

The current study was carried out in two sections. Firstly, the effect of contact time, adsorbent dosage, and sulfur-compound concentration was studied. In the second part, the obtained results were modeled with

various isotherm and kinetics models to clarify the mechanism of sulfur-species elimination.

#### Effect of contact time and sulfur concentration

Like any chemical reactions, time is addressed as one of the most important parameters, affecting the performance of the whole system. Generally, to achieve an efficient balance between adsorbent and adsorbate, adequate contact time must be considered in adsorption processes. Accordingly, the effect of contact time on sulfur removal was examined at two different concentration levels (150 and 400 ppm) and in the time period of 0-150 min. The dosage of polyacrylonitrile/Ag nanofiber composite was maintained at 0.02 g. The findings are exhibited in Figure 4. Based on Figure 4a, it

indicates that by increasing the contact time, the removal efficiency tends to improve, and reached the maximum value of 44% and 22.5% for sulfur concentrations of 150 and 400 ppm, respectively. Also, Figure 4b shows the concentration of sulfur at different time intervals, and it can be figured out that the final concentration of sulfur reached 84 and 310 ppm for initial concentrations of 150 and 400 ppm, respectively.

A closer look at the curve (Fig. 4a) reveals that at initial step of adsorption process the removal efficiency increased rapidly, and then experienced a smooth slope

to reach an equilibrium at 90 min. Further increase in the reaction time from 90 to 150 min had no effect on the performance of the system. So, optimum contact time was found 90 min. These results could be attributed to the fact that polyacrylonitrile/Ag nanofiber composite has abundant vacant sites at initial step of the adsorption, leading to a quick enhancement in the removal efficiency [31]. However, these sites are occupied by sulfur molecules through time, so the removal efficiency slope would decrease until reach a situation in which the rate of the adsorption and

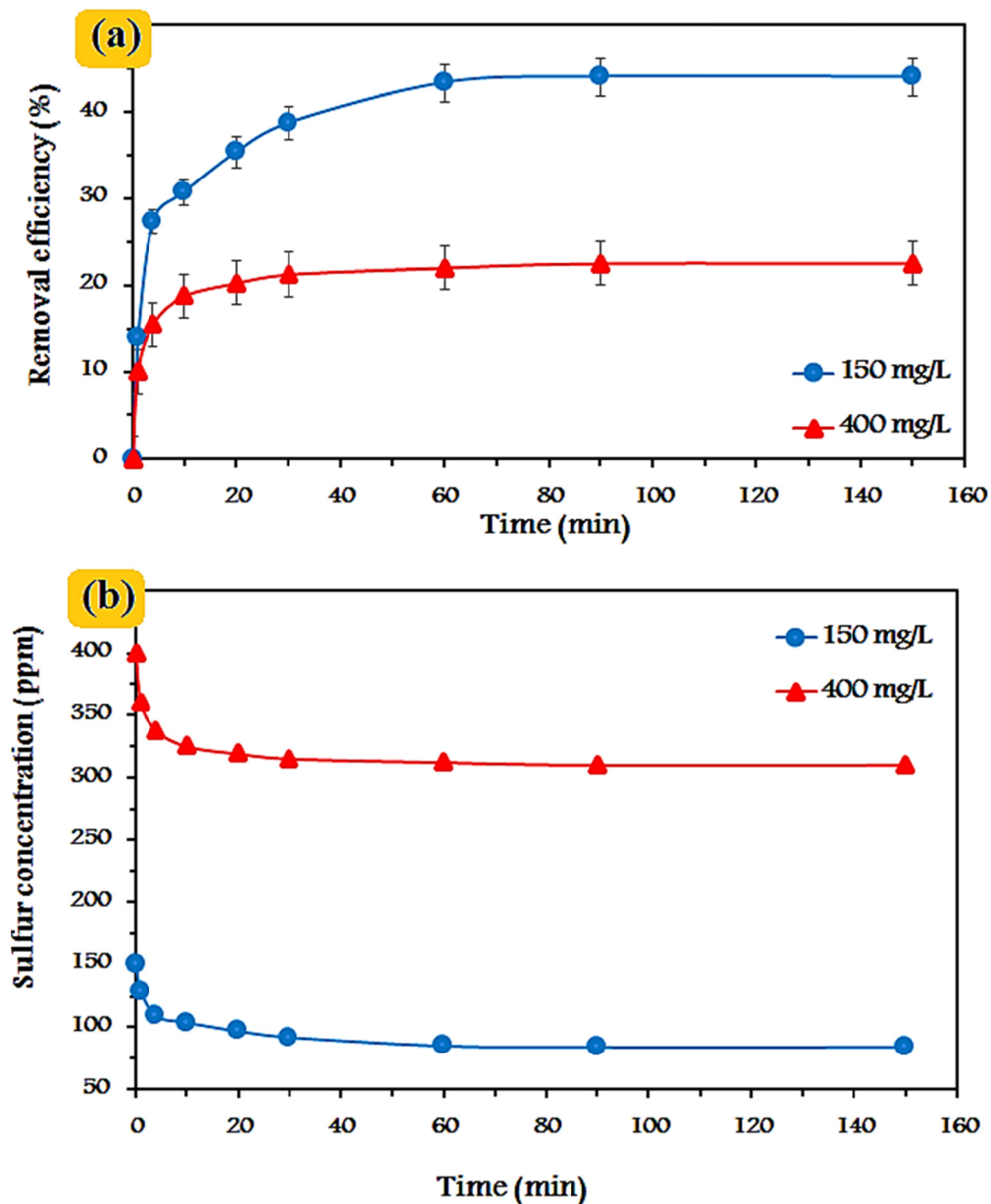
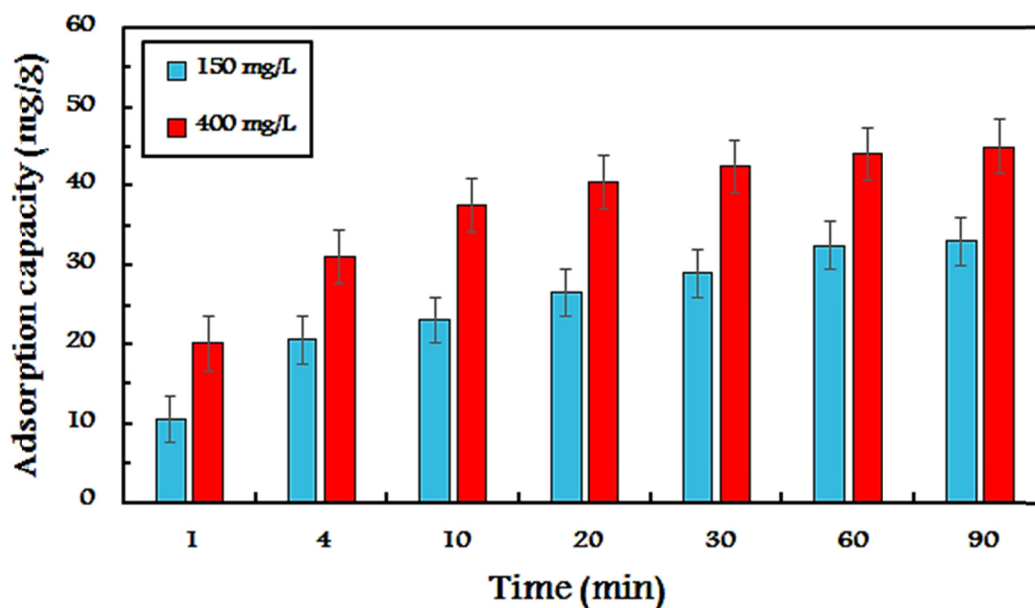


Figure 4. Effect of contact time (a), and sulfur concentration in different time intervals (b).



**Figure 5.** The fluctuations of adsorption capacity by time changes for sulfur adsorption (150 and 400 ppm) by polyacrylonitrile/Ag nanofiber composite.

desorption from the surface of the adsorption are identical (occurred at 90 min). Similar deductions have also reported by previous scholars.

Figure 4a also demonstrates that initial sulfur concentration is vitally important because it directly affects the removal efficiency of the pollutants. The sulfur removal efficiency at 150 ppm was 1.95 times greater than that of 400 ppm, proving that lower sulfur concentration is more beneficial for adsorption technique. Since polyacrylonitrile/Ag nanofiber dosage was constant during the experiments, there are limited number of available sites on the adsorption, and logically lower sulfur concentration might end in higher removal efficiency. Moreover, the fluctuations of adsorption capacity by time variations were calculated, and is shown in Figure 5. At both concentration, adsorption capacity was increased by increasing the time contact, and the maximum adsorption capacity was 33 mg/g for 150 ppm and 45 mg/g for 400 ppm. The greater adsorption capacity at higher sulfur concentration is due to greater gradient concentration at 400 ppm than 150 ppm which forces sulfur molecules to go toward adsorbent surface, and consequently a greater adsorption capacity [32].

#### **Effect of adsorbent dosage**

Adsorbent dosage is defined as the mass of material that is required to reach the desired sulfur removal efficiency. The importance of this parameter is also

attributed to its direct influence on the final cost of desulfurization. Accordingly, in the current study the effect of polyacrylonitrile/Ag nanofiber dosage on the sulfur removal and also adsorption capacity was investigated. The experimental findings are illustrated in Figure 6. The adsorbent dosage was ranging from 0.02 to 0.4g, and sulfur concentration was 400 mg/L. The figure clearly proves that by increasing the adsorbent dosage, the removal efficiency excelled. Numerically, the removal efficiency improved from 7.75% to 77.75% by increasing polyacrylonitrile/Ag nanofiber dosage from 0.02 to 0.40 gr, respectively. It states that higher dosage of adsorbent is beneficial in terms of removal efficiency. The main reason for such behavior might be attributed to the fact that by increasing the adsorbent dosage, more vacant sites become available for adsorbate molecules [33]. Zheng et al. [34] also reported that desulfurization performance exhibited better efficiency by increasing the Ag-based adsorbent.

In contrast, the adsorption capacity decreased from 46.50 to 23.33 mg/g by increasing the adsorbent dosage from 0.02 to 0.4 g, respectively. Unlike removal efficiency, it can be observed that adsorption capacity owns higher values at lower dosage of polyacrylonitrile/Ag nanofiber. This observation is due to the gradient between adsorbent dosage and adsorbate molecules. In other words, at low adsorbent dosage, the gradient between adsorbent and adsorbate is of high that sulfur molecules are forces to move toward

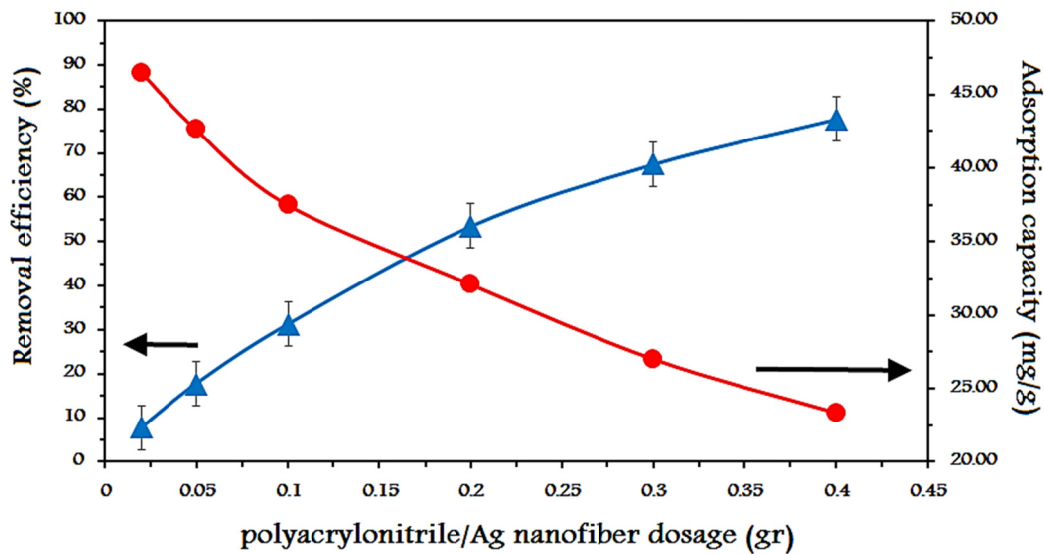


Figure 6. the effect of adsorbent dosage on the removal efficiency and adsorption capacity.

polyacrylonitrile/Ag surface, resulting in higher adsorbent capacity. By increasing the adsorbent dosage, adsorbate molecules face a plenty number of empty sites that are somehow redundant, and remain vacant after the accomplishment of the adsorption process [32].

**Isotherm of adsorption**

The isothermal equations of a specific adsorbent indicate the adsorption properties of the adsorbent, which play a significant role in designing the adsorption process. In addition, adsorption isotherm is considered as one of the important factors in designing the system which describes the interactions between the adsorbent and adsorbate molecules. In fact, isotherm equation attempts to provide a relationship between adsorbent and adsorbate in the equilibrium state under constant temperature and pH. Up to now, countless isotherms have been proposed by researchers that among them, Langmuir, Freundlich, Dubinin-Radushkevich, and Temkin are known as the most common ones.

Langmuir equation is employed for single layer adsorptions on a homogeneous surface, on the other hand Freundlich isotherm model is suitable for multilayer surface adsorption in heterogeneous systems. Linear forms of Langmuir and Freundlich models are expressed as [11,12]:

$$\frac{C_e}{q_e} = \frac{1}{K_L q_{max}} + \frac{1}{q_{max}} C_e$$

$$\ln q_e = \ln K_f + \frac{1}{n} \ln C_e$$

where  $K_L$  (L/mg) is the Langmuir equilibrium

constant which describe the dependence of binding sites with the adsorbate and  $q_{max}$  (mg/g) is the single layer capacity referred to the amount of sulfur required to engross all the available sites of nanocomposite.  $K_f$  is the Freundlich constant related to adsorption capacity and  $n$  is the heterogeneity coefficient and  $1/n$  is a measure of intensity of adsorption.

The constant parameters and linear plots of isotherms are summarized in Table 1 and illustrated in Figure 7, respectively. The most appropriate adsorption isotherm was selected by the coefficient of determination ( $R^2$ ) in which as its value gets closer to one, the model could satisfactorily describe the experimental findings. By comparing the  $R^2$  value of the examined isotherms, it can be stated that Freundlich assumptions was better than Langmuir equation to expound the results. The appropriateness of Freundlich model is indicative of the fact that sulfur molecules tend to aggregate over polyacrylonitrile/Ag surface to form multilayers and the surface acts as a heterogeneous media. The  $n$  parameter of Freundlich model was great than one, signifying that the whole process was favorable, and sulfur molecules tend to establish chemical bonds via chemical adsorptions. Although Freundlich was the best model, high  $R^2$  value of Langmuir could not be ignored. To elucidate the process, dimensionless equilibrium parameter ( $R_L$ ) can be employed which is written as [35]:

$$R_L = \frac{1}{1 + K_L C_0}$$

Table 1. Calculated isotherms parameters for sulfur species adsorption by electrospun polyacrylonitrile/Ag composite.

Isotherm	Parameter	Value
Langmuir	$q_m$	59.88
	$K_L$	0.0068
	$R^2$	0.9688
	$R_L$	< 1
Freundlich	$K_f$	2.71
	$n$	2.11
	$1/n$	0.4746
	$R^2$	0.9900
DR	$q_m$	41.93
	$\beta$	0.0009
	$R^2$	0.8273
Temkin	$b$	187.0071
	$A$	0.04461
	$R^2$	0.9648

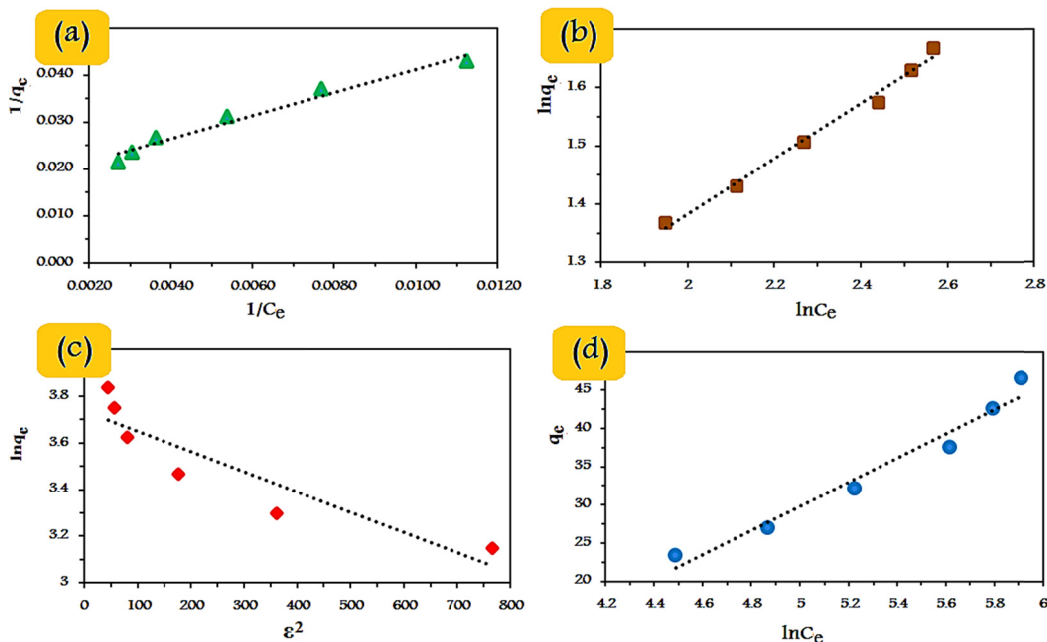


Figure 7. The linear plots if isotherm models: (a) Langmuir, (b) Freundlich, (c) D-R, and (d) Temkin.

Based on the  $R_L$  value it can be said that the adsorption is favorable, unfavorable, linear, or irreversible. Sulfur adsorption by polyacrylonitrile/Ag composite showed the  $R_L$  value of lower than unity, indicating that the process is favorable. Thus, the results suggest that the whole adsorption is governed by Freundlich assumptions, however, in some regions of the adsorbent monolayer disposition of sulfur molecules is expected.

For further investigation, Dubinin-Radushkevich was

utilized that has been employed in many equilibrium studies. Micropore volume filling is assumed as the adsorptive mechanism and the model is based on the potential theory. Of advantages of Dubinin-Radushkevich, it can be mentioned that this model is not only for homogenous surfaces, and also do not intend constant adsorption potential. The Dubinin-Radushkevich (D-R) linear equation could be written as [11]:

$$\ln q_e = \ln q_m - \beta \epsilon^2$$

$$\varepsilon = RT \ln \left( 1 + \frac{1}{C_e} \right)$$

where  $q_e$  (mg/g) is the amount of sulfur compounds adsorbed per unit mass of polyacrylonitrile/Ag at equilibrium;  $q_{\max}$  (mg/g) is the maximum adsorption capacity of polyacrylonitrile/Ag;  $\beta$  ( $\text{mol}^2/\text{kJ}^2$ ) is a constant related to the adsorption energy; and  $\varepsilon$  (kJ/mol) is the adsorption potential. The constant parameters are obtained from linear plot of  $\ln q_e$  versus  $\varepsilon^2$ .

Temkin isotherm model was proposed based on the adsorption energy in which states that adsorption energy tends to decreased linearly by occupation of the empty sites of polyacrylonitrile/Ag by sulfur [36]. This model is written as:

$$q_e = \frac{RT}{b} \ln A + \frac{RT}{b} \ln C_e$$

where  $b$  is called Temkin constant, relating to the heat of adsorption process, and  $A$  is Temkin isotherm constant. The parameters are calculated from slope and intercept of linear plot of  $q_e$  versus  $\ln C_e$ .

Figure 7 and Table 1 show the linear plot and constants of the D-R and Temkin isotherms, respectively. According to the obtained  $R^2$  values, it can be stated that Temkin was more suitable than D-R model. The appropriateness of Temkin isotherm over D-R model could also be figured out by the semi-large difference between the maximum experimental adsorption capacity and D-R  $q_m$  value. Furthermore, D-R isotherm could provide substantial information regarding the adsorption energy, which is calculated by:

$$E = \frac{1}{\sqrt{2\beta}}$$

where  $E$  is the adsorption energy (kJ/mol). Generally, according to  $E$  value adsorption isotherm is categorized into physical adsorption and chemical adsorption. Physical sorption processes have low adsorption energy that is usually lower than 8 kJ/mol [37]. In the current study for sulfur adsorption by polyacrylonitrile/Ag composite, the  $E$  value was found 23.57 kJ/mol,

demonstration chemical interactions between adsorbent and adsorbate. Considering all four isotherms, it can be deduced that the order of isotherm fitting is as follows:

$$\text{Freundlich} > \text{Langmuir} > \text{Temkin} > \text{D-R}$$

Therefore, it can be concluded that sulfur adsorption follows Freundlich assumptions. Finally, as shown in Table 2, a comparison was made between the desulfurization performances of the nanocomposites developed in the present study with those of the previous reports. As shown, the adsorption capacity of nanofiber described in this work is considerably higher than those in previous reports, which demonstrates its higher adsorbent ability for desulfurizing the gas condensate.

### Kinetic studies

The rate of chemical reactions states how fast the system is working, and could highly affect the in-situ operational parameters. Accordingly, kinetic models are categorized into two different groups, providing different insights regarding the reactions. The first group, called solute concentration-based, considers the fluctuation of the adsorbate concentration regardless of the adsorbent presence. This approach intends the initial and final concentration of the sulfur compound in the solution. In another perspective, the mass of the adsorbent and sulfur concentration changes is considered, known as adsorbent dosage-based models.

Among solute concentration-based models, first order and second order equations have been utilized in many investigations. First and second order rate equations are expressed as follow [38]:

$$\ln C_t = \ln C_0 - K_1 t$$

$$\frac{1}{C_t} = K_2 t + \frac{1}{C_0}$$

where  $C_t$  (mg/L) and  $C_0$  (mg/L) refer to concentration of sulfur at time  $t$  and initial sulfur concentration, respectively.  $K_1$  and  $K_2$  are the constant parameters of

**Table 2.** Comparison of the adsorption capacity of the synthesized PAN/Ag nanofibers with other works in desulfurization process

Adsorbent	Adsorption capacity (mg/g adsorbent)	Reference
30 wt% Ni/SBA-15 with a low-sulfur diesel	1.7	[44]
Nickel nanoparticles inside the mesopores of MCM-41 b	1.67	[45]
Pelletized Ce-Y zeolites	0.86	[46]
30 wt% Ni/SBA-15	1.7	[47]
Ni-based adsorbent	14.2	[48]
ACFH-Cu <sup>+</sup>	19.0	[49]
Graphene-like boron nitride	28.17	[50]
PAN-ABS-Pb	31.4	[10]
PAN/Ag nanofiber	102	In this work

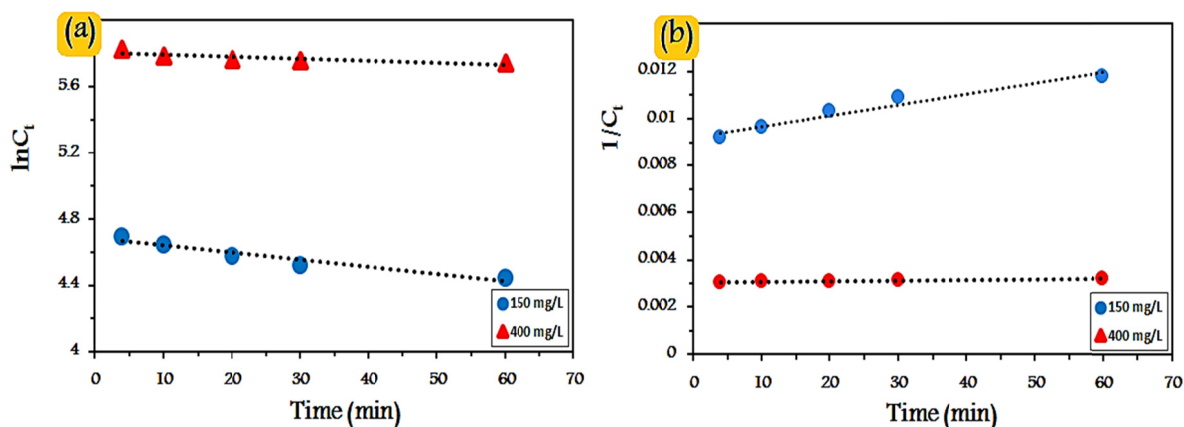


Figure 8. Linear plot of first order (a) and second order (b) models.

Table 3. The values of constant parameters of first order and second order models.

Initial Sulfur concentration	First order model		Second order model	
	R <sup>2</sup>	K <sub>1</sub>	R <sup>2</sup>	K <sub>2</sub>
150	0.9352	0.0043	0.9617	5E-05
400	0.6971	0.0012	0.9471	3E-06

the model, and found by linear plot of  $\ln C_t$  vs.  $t$  and  $\frac{1}{C_t}$  vs.  $t$  for first order and second order, respectively. Results are summarized in Table 3 and Figure 8.

According to the obtained results, it could be seen that at low sulfur compound (150 mg/L) both first and second models are almost well since they have R<sup>2</sup> values of greater than 0.9. However, at higher sulfur compound concentration (400 mg/L), it seems that first order model could not be appropriate to expound the removal process mechanism. Hence, it is generally suggested that sulfur compound removal by polyacrylonitrile/Ag composite follows the second order model.

Up to now, various adsorbent dosage-based kinetics models have been proposed by many researchers, considering different assumptions. Among them, pseudo-first order (PFO) and pseudo-second order (PSO) are the most popular equations and were selected to approve the adsorption kinetic. This two models are generally expressed as [39]:

$$\ln(q_e - q_t) = -K_1 t + \ln q_e$$

$$\frac{t}{q_t} = \frac{1}{K_2 q_e^2} + \frac{1}{q_e} t$$

where  $q_e$  (mg/g) and  $q_t$  (mg/g) are the polyacrylonitrile/Ag composite adsorption capacities at equilibrium (min) and at time  $t$  (min), respectively.  $K_1$  (min<sup>-1</sup>) and  $K_2$  (g mg<sup>-1</sup> min<sup>-1</sup>) are the pseudo-first and the pseudo-second order rate constants.

The kinetic parameters for the PFO and the PSO kinetic models were calculated from the intercept and

slope of linear plots presented in Figure 9, and the constant parameters are summarized in Table 4. Validity of the models could be verified by R<sup>2</sup> values and  $q_e$ . In view of R<sup>2</sup> values, it shows that PSO demonstrated a very high value close to unity compared to PFO. For instance, for 400 ppm, R<sup>2</sup> value for PSO was 0.9998; however, of PFO it was 0.9656. It is indicative of the fact that PSO is more suitable to describe the equilibrium data. It must not be ignored that PFO also exhibited high R<sup>2</sup> values which were both greater than 0.95. So, more discussion could be carried out by the adsorption capacities obtained from experimental ( $q_{e, \text{experimental}}$ ) result and kinetic models ( $q_{e, \text{kinetic}}$ ). Generally, no large difference between these two values must be observed. In case of 400 rpm, for instance,  $q_{e, \text{experimental}}$  was 45.10 mg/g, and  $q_{e, \text{kinetic}}$  for PFO and PSO were 17.47 and 45.87 mg/g, respectively. Clearly, the value of  $q_{e, \text{experimental}} - q_{e, \text{kinetic}}$  was negligible for PSO. Therefore, it could be concluded that sulfur compound adsorption by polyacrylonitrile/Ag composite obeyed PSO assumption.  $K_2$  value is a sign of equilibrium state arrival [40], and in the current study,  $K_2$  value for 400 rpm was 1.47 times higher than that of 150 ppm. This occurrence may attribute to the number of sulfur compound molecules in the solution in which at 400 ppm is higher than 150 ppm. Appropriateness of PSO over PFO for sulfur compound adsorption by polyacrylonitrile/Ag composite has already been expected since PFO is frequently applied for the initial steps of adsorption, and it is good almost for physical

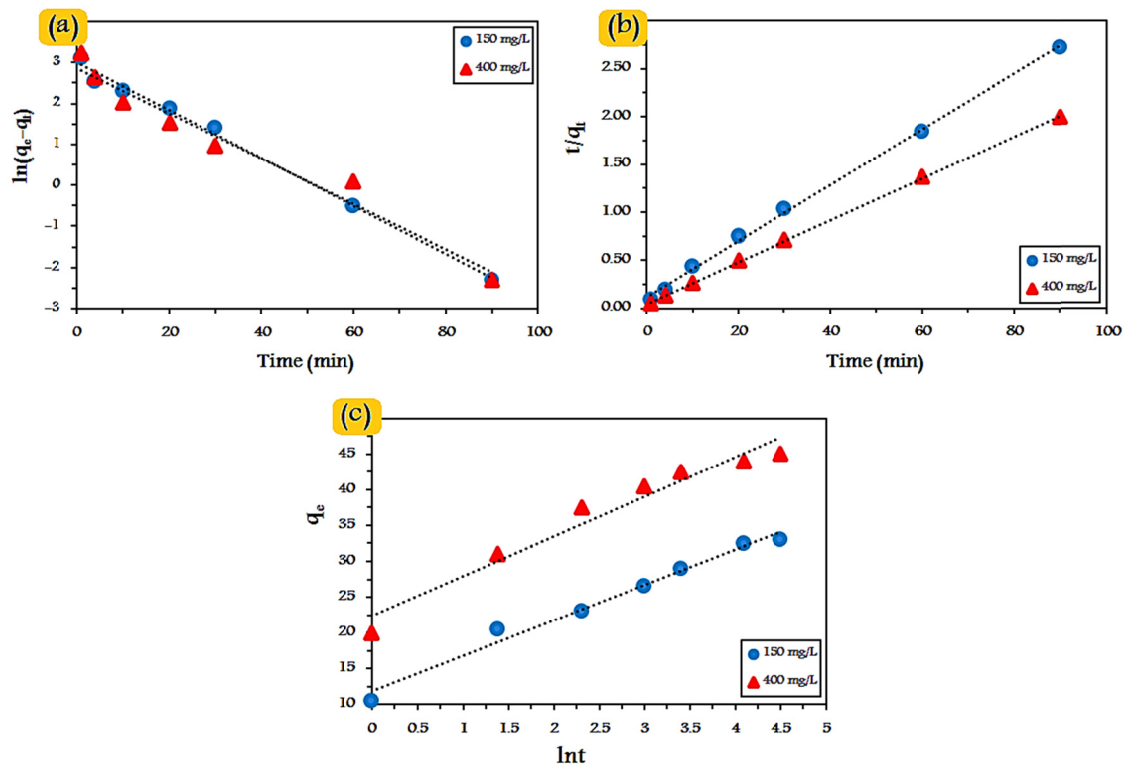


Figure 9. Linear plots of pseudo-first order (a), pseudo-second order (b), and Elovich (c) for sulfur compound adsorption by polyacrylonitrile/Ag.

Table 4. The constant parameters of examined kinetics models for sulfur compound removal by polyacrylonitrile/Ag

Kinetic model		150 ppm	400 ppm
Pseudo-first order	Equation	$y = 0.0585x + 3.0033$	$y = -0.0552x + 2.8613$
	$K_1$	0.0585	0.0552
	$q_e$ , kinetic	20.14	17.47
	$q_e$ , experimental	33.10	45.10
	$R^2$	0.9943	0.9656
Pseudo-second order	Equation	$y = 0.0292x + 0.1172$	$y = 0.0218x + 0.0448$
	$K_2$	0.0072	0.0106
	$q_e$ , kinetic	34.24	45.87
	$q_e$ , experimental	33.10	45.10
	$R^2$	0.9982	0.9998
Elovich	Equation	$y = 4.954x + 11.78$	$y = 5.5381x + 22.435$
	$\alpha$	46.437	318.182
	$\beta$	0.2018	0.1805
	$R^2$	0.9823	0.9531

adsorption [32,41]. It is believed that functional groups on polyacrylonitrile/Ag are capable of providing chemical bonds with sulfur compounds via chemisorption.

Elovich is also known as a practical adsorption kinetic model to describe chemical reaction mechanism [42]. This models implies a multilayer adsorption, and is

expressed as [43]:

$$q_e = \frac{1}{\beta} \ln t + \frac{1}{\beta} \ln (\alpha\beta)$$

where  $\alpha$  (g/mg) is the constant and  $\beta$  (mg/g min) is the initial adsorption. The plot and parameters are shown in Figure 9 and Table 4.

For both concentration, the  $R^2$  value was extremely

high (0.9823 and 0.9531 for 150 and 400 ppm, respectively) suggesting that Elovich assumptions may well-fitted the sulfur compound adsorption. Considering all three kinetics models, it is fair to suggest that both PSO and Elovich are able to describe the sorption process. It demonstrates that sulfur molecules tend to create chemical bonds with heterogeneous surface of polyacrylonitrile/Ag.

#### Efficiency studies

The experimental adsorption column was employed to investigate the efficiency of polyacrylonitrile/Ag composite nanofibers for the removal of sulfur

compounds from natural gas condensate. For this purpose, a glass column of 0.5 cm in diameter was used with a glass wool placed at the bottom and filled with 20 g of the synthesized nanocomposite. At the top of the glass column, a tank containing 5 liters of gas condensate was placed with the total sulfur content of 1250 mg/L with a regulator valve at a flow rate of 6 mL/min as shown in Figure 10a. After passing 2160 mL of gas condensate, the  $C/C_0$  ratio approached a value of 1, indicating that the adsorbent is saturated and needs to be recovered, the plot of this results are depicted in Figure 10b.

In order to conduct retrieval studies, 0.02 gr of

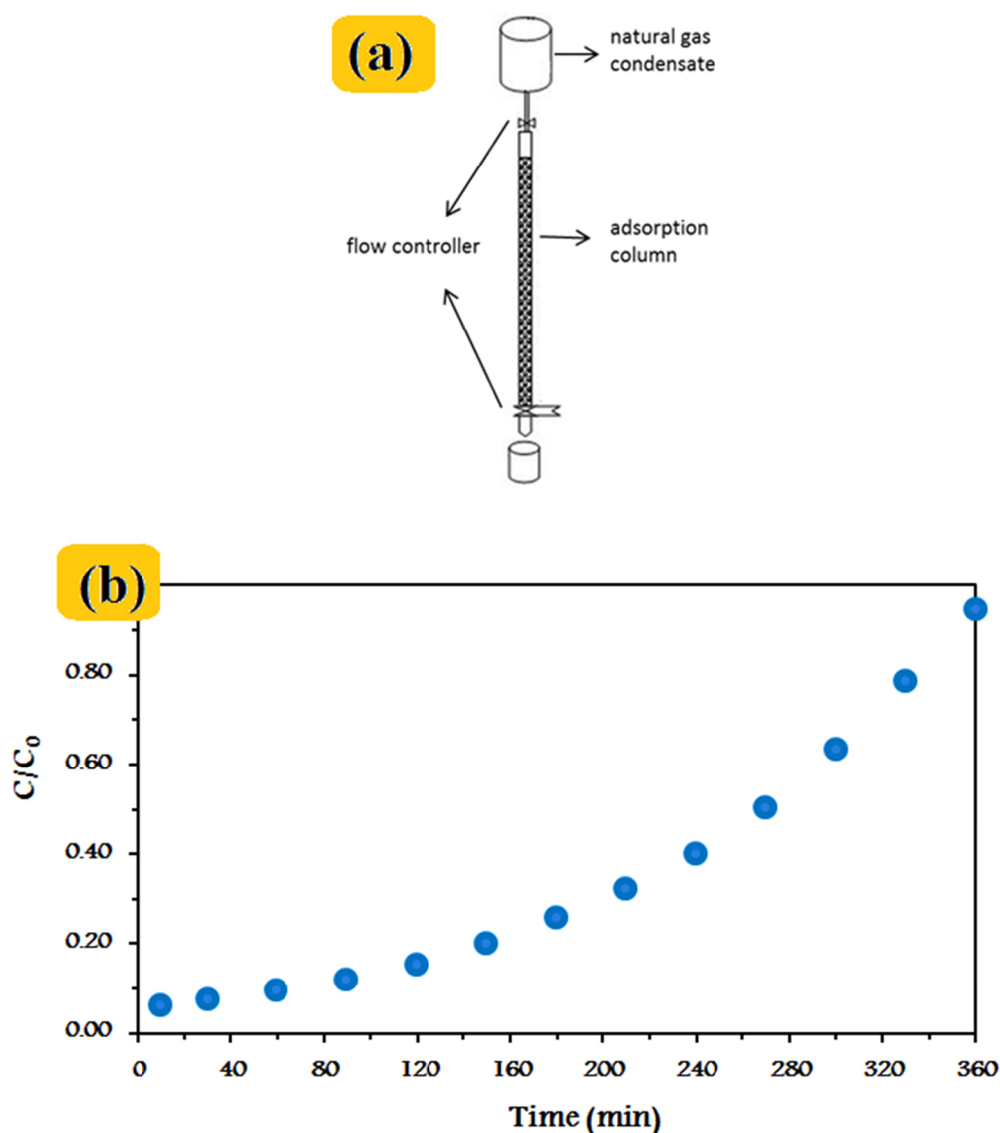


**Figure 10.** (a) Glass column with 0.5 cm diameter and (b) adsorption of sulfur using column packed with synthesized nanocomposite nanofiber (adsorbent= 20 g, initial sulfur content= 1250 mg/L, flow rate= 6 ml/min).

polyacrylonitrile/Ag nanocomposites was placed in 10 mL of gas condensate with the total sulfur 150 mg/L and the total sulfur content was reached to 90 mg/l (40% adsorption) after 30 minutes. Then, the nanocomposites were placed under hydrogen gas purge for 10 minutes and again the same nanocomposites were inserted into 10 mL of gas condensate with 150 mg/L total sulfur content, and the total sulfur content was reached to 110 mg/L (26.7% adsorption) after 30 minutes. Based on the results, the nanofibers were recovered and the sulfur compounds were adsorbed again by the nanofibers under the hydrogen gas purge, indicating their good recoverable behavior.

Finally, it is fair to suggest that the prepared material in the current study for desulfurization, has an appropriate removal/adsorption efficiency as well as the synthesis procedure is simple and cost-effective.

### Conclusion

In this work, polyacrylonitrile/silver nanoparticles nanocomposite was prepared for the first time to adsorb sulfur contents in gas condensates. XRD peaks revealed that Ag nanoparticles were available in the composite and SEM images showed that the fibres were synthesized very well. These nanofibers are connected to each other at different points, which are not completely separate. It was found that by increasing the contact time and adsorbent dosage, desulfurization enhanced and got higher performance. Furthermore, lower concentration of sulfur compounds was beneficial in terms of adsorption/removal. Based on the results in adsorption isotherms, the adsorption of sulfur compounds was followed by Freundlich isotherm. Such behavior was ascribed to heterogeneous nature of the polyacrylonitrile/silver nanoparticles that tend to establish chemical bonds with the sulfur compounds. The energy of the adsorption calculated by Dubinin-Radushkevich equation also stated identical deduction by showing the process to be chemical-based sorption. Further, kinetic studies indicated that desulfurization by using nanocomposite follows pseudo-second-order kinetics. Furthermore, the adsorbent column studies confirmed the usability of desulfurization process with polyacrylonitrile/Ag nanocomposite with a good recovery performance. Finally, the unique adsorbent ability and simple synthesis makes it a good candidate for industrial applications.

### Acknowledgment

The present work was supported by the South Pars Gas Complex. We would like to thank the SPGC for providing laboratory facilities.

### References

- Dong S., Li M., Firoozabadi A. Effect of salt and water cuts on hydrate anti-agglomeration in a gas condensate system at high pressure. *Fuel*, **210**: 713–20 (2017).
- Ke T., Xin H. Deep desulfurization of model gasoline by adsorption on mesoporous CeMCM-41. *Pet. Sci. Technol.*, **28**: 573–81 (2010).
- Samadi M., Zarenezhad B. Extension of gas adsorption models to liquid diesel fuel desulfurization: Validity and predictability. *Pet. Sci. Technol.*, **34**: 1826–32 (2016).
- Leong M., Chian K., Mhaisalkar P., Ong W., Ratner B. Effect of electrospun poly(D,L-lactide) fibrous scaffold with nanoporous surface on attachment of porcine esophageal epithelial cells and protein adsorption. *J. Biomed. Mater. Res. A*, **89**: 1040–8 (2009).
- Yang RT., Hernández-Maldonado AJ., Yang FH. Desulfurization of transportation fuels with zeolites under ambient conditions. *Science (80-. )*, **301**: 79–81 (2003).
- Bakhtiari G., Abdouss M., Bazmi M., Royaei SJ. Optimization of sulfur adsorption over Ag-zeolite nano-adsorbent by experimental design method. *Int. J. Environ. Sci. Technol.*, **13**: 803–12 (2016).
- Tang X., Hu T., Li J., Wang F., Qing D. Deep desulfurization of condensate gasoline by electrochemical oxidation and solvent extraction. *RSC Adv.*, **5**: 53455–61 (2015).
- Tella AC., Owalude SO., Olatunji SJ., Oloyede SO., Ogunlaja AS., Bourne SA. Synthesis, crystal structure and desulfurization properties of zig-zag 1D coordination polymer of copper (II) containing 4-methoxybenzoic acid ligand. *J. Sulfur Chem.*, **39**: 588–606 (2018).
- Li C.-J., Li Y.-J., Wang J.-N., Zhao L., Cheng J. Ag<sup>+</sup>-loaded polystyrene nanofibrous membranes preparation and their adsorption properties for thiophene. *Chem. Eng. J.*, **222**: 419–25 (2013).
- Allafchian AR., Gholamian M., Mohammadi J. Desulfurization of gasoline using acrylonitrile electrospun nanofibers and lead nanoparticles. *Int. J. Environ. Sci. Technol.*, **14**: 1489–96 (2017).
- Khadir A., Negarestani M., Mollahosseini A. Sequestration of a non-steroidal anti-inflammatory drug from aquatic media by lignocellulosic material (*Luffa cylindrica*) reinforced with polypyrrole: study of parameters, kinetics, and equilibrium. *J. Environ. Chem. Eng.*, **8**: 103734 (2020).
- Khadir A., Negarestani M., Ghiasinejad H. Low-cost sisal fibers/polypyrrole/polyaniline biosorbent for sequestration of reactive orange 5 from aqueous solutions. *J. Environ. Chem. Eng.*, **8**: 103956 (2020).
- Shu C., Yanwei W., Hong L., Zhengzheng P., Kangde Y. Synthesis of carbonated hydroxyapatite nanofibers by mechanochemical methods. *Ceram. Int.*, **31**: 135–8 (2005).
- Yu J., Yu H., Cheng B., Zhao X., Zhang Q. Preparation and photocatalytic activity of mesoporous anatase TiO<sub>2</sub> nanofibers by a hydrothermal method. *J. Photochem. Photobiol. A Chem.*, **182**: 121–7 (2006).
- Malwal D., Gopinath P. Efficient adsorption and antibacterial properties of electrospun CuO-ZnO composite nanofibers for water remediation. *J. Hazard. Mater.*, **321**: 611–21 (2017).

16. Huang Z-M., Zhang Y-Z., Kotaki M., Ramakrishna S. A review on polymer nanofibers by electrospinning and their applications in nanocomposites. *Compos. Sci. Technol.*, **63**: 2223–53 (2003).
17. Mollahosseini A, Rastegari M., Hatefi N. Electrospun Polyacrylonitrile as a New Coating for Mechanical Stir Bar Sorptive Extraction of Polycyclic Aromatic Hydrocarbons from Water Samples. *Chromatographia*, **83**: 549–58 (2020).
18. Habiba U., Afifi AM., Salleh A., Ang BC. Chitosan/(polyvinyl alcohol)/zeolite electrospun composite nanofibrous membrane for adsorption of Cr<sup>6+</sup>, Fe<sup>3+</sup> and Ni<sup>2+</sup>. *J. Hazard. Mater.*, **322**: 182–94 (2017).
19. Zhang S., Shi Q., Korfiatis G., Christodoulatos C., Wang H., Meng X. Chromate removal by electrospun PVA/PEI nanofibers: Adsorption, reduction, and effects of co-existing ions. *Chem. Eng. J.*, **387**: 124179 (2020).
20. Lee C-G., Javed H., Zhang D., Kim J-H., Westerhoff P., Li Q., Alvarez PJJ. Porous electrospun fibers embedding TiO<sub>2</sub> for adsorption and photocatalytic degradation of water pollutants. *Environ. Sci. Technol.*, **52**: 4285–93 (2018).
21. Habiba U., Siddique TA., Li Lee JJ., Joo TC., Ang BC., Afifi AM. Adsorption study of methyl orange by chitosan/polyvinyl alcohol/zeolite electrospun composite nanofibrous membrane. *Carbohydr. Polym.*, **191**: 79–85 (2018).
22. Dou X., Wang Q., Li Z., Ju J., Wang S., Hao L., Sui K., Xia Y., Tan Y. Seaweed-Derived Electrospun Nanofibrous Membranes for Ultrahigh Protein Adsorption. *Adv. Funct. Mater.*, **29**: 1905610 (2019).
23. Thielke MW., Bultema LA., Brauer DD., Richter B., Fischer M., Theato P. Rapid Mercury (II) removal by electrospun sulfur copolymers. *Polymers (Basel)*, **8**: 266 (2016).
24. Mukwevho N., Gusain R., Fosso-Kankeu E., Kumar N., Waanders F., Ray SS. Removal of naphthalene from simulated wastewater through adsorption-photodegradation by ZnO/Ag/GO nanocomposite. *J. Ind. Eng. Chem.*, **81**: 393–404 (2020).
25. Yang Y., Li H., Hou F., Hu J., Zhang X., Wang Y. Facile synthesis of ZnO/Ag nanocomposites with enhanced photocatalytic properties under visible light. *Mater. Lett.*, **180**: 97–100 (2016).
26. Li J., Yang S., Du Z., Wang R., Yuan L., Wang H., Wu Z. Quantitative analysis of ammonia adsorption in Ag/AgI-coated hollow waveguide by mid-infrared laser absorption spectroscopy. *Opt. Lasers Eng.*, **121**: 80–6 (2019).
27. Zaheer Z., AL-Asfar A., Aazam ES. Adsorption of methyl red on biogenic Ag@Fe nanocomposite adsorbent: Isotherms, kinetics and mechanisms. *J. Mol. Liq.*, **283**: 287–98 (2019).
28. Satokawa S., Kobayashi Y., Fujiki H. Adsorptive removal of dimethylsulfide and t-butylmercaptan from pipeline natural gas fuel on Ag zeolites under ambient conditions. *Appl. Catal. B Environ.*, **56**: 51–6 (2005).
29. Nair S., Tatarchuk BJ. Supported silver adsorbents for selective removal of sulfur species from hydrocarbon fuels. *Fuel*, **89**: 3218–25 (2010).
30. Sun X., Tatarchuk BJ. Photo-assisted adsorptive desulfurization of hydrocarbon fuels over TiO<sub>2</sub> and Ag/TiO<sub>2</sub>. *Fuel*, **183**: 550–6 (2016).
31. Mirjavadi ES., M.A.Tehrani R., Khadir A. Effective adsorption of zinc on magnetic nanocomposite of Fe<sub>3</sub>O<sub>4</sub>/zeolite/cellulose nanofibers: kinetic, equilibrium, and thermodynamic study. *Environ. Sci. Pollut. Res.*, **26**: 33478–33493 (2019).
32. Mollahosseini A., Khadir A., Saeidian J. Core-shell polypyrrole/Fe<sub>3</sub>O<sub>4</sub> nanocomposite as sorbent for magnetic dispersive solid-phase extraction of Al<sup>3+</sup> ions from solutions: investigation of the operational parameters. *J. Water Process Eng.*, **29**: 100795 (2019).
33. Ghenaatgar A., M.A.Tehrani R., Khadir A. Photocatalytic degradation and mineralization of dexamethasone using WO<sub>3</sub> and ZrO<sub>2</sub> nanoparticles: Optimization of operational parameters and kinetic studies. *J. Water Process Eng.*, **32**: 100969 (2019).
34. Zheng M., Hu H., Ye Z., Huang Q., Chen X. Adsorption desulfurization performance and adsorption-diffusion study of B<sub>2</sub>O<sub>3</sub> modified Ag-CeO<sub>x</sub>/TiO<sub>2</sub>-SiO<sub>2</sub>. *J. Hazard. Mater.*, **362**: 424–35 (2019).
35. Khadir A., Mollahosseini A., Tehrani RMA., Negarestani M. A Review on Pharmaceutical Removal from Aquatic Media by Adsorption: Understanding the Influential Parameters and Novel Adsorbents BT - Sustainable Green Chemical Processes and their Allied Applications. (Inamuddin , Asiri Abdullah ed.), Springer International Publishing, Cham, pp.207–65 (2020).
36. Nimibofa A., Ebelegi A., Donbebe W. Modelling and Interpretation of Adsorption Isotherms. *Hindawi J. Chem.*, **Volume 201**: 11 pages (2017).
37. Mohammadi A., Khadir A., Tehrani RMA. Optimization of nitrogen removal from an anaerobic digester effluent by electrocoagulation process. *J. Environ. Chem. Eng.*, **7**: 103195 (2019).
38. Khadir A., Negarestani M., Motamedi M. Optimization of an electrocoagulation unit for purification of ibuprofen from drinking water: effect of conditions and linear/non-linear isotherm study. *Sep. Sci. Technol.*, (2020).
39. Khadir A., Motamedi M., Negarestani M., Sillanpää M., Sasani M. Preparation of a nano bio-composite based on cellulose biomass and conducting polymeric nanoparticles for ibuprofen removal: Kinetics, isotherms, and energy site distribution. *Int. J. Biol. Macromol.*, **162**: 663–677 (2020).
40. Turk Sekulic M., Boskovic N., Milanovic M., Grujic Letic N., Gligoric E., Pap S. An insight into the adsorption of three emerging pharmaceutical contaminants on multifunctional carbonous adsorbent: Mechanisms, modelling and metal coadsorption. *J. Mol. Liq.*, **284**: 372–82 (2019).
41. Tran HN., You S-J., Hosseini-Bandegharai A., Chao H-P. Mistakes and inconsistencies regarding adsorption of contaminants from aqueous solutions: A critical review. *Water Res.*, **120**: 88–116 (2017).
42. Wu F-C., Tseng R-L., Juang R-S. Characteristics of Elovich equation used for the analysis of adsorption kinetics in dye-chitosan systems. *Chem. Eng. J.*, **150**: 366–73 (2009).
43. Li C., Chen D., Ding J., Shi Z. A novel hetero-exopolysaccharide for the adsorption of methylene blue from aqueous solutions: Isotherm, kinetic, and mechanism

- studies. *J. Clean. Prod.*, **265**: 121800 (2020).
44. Park JG., Ko CH., Yi KB., Park J-H., Han S-S., Cho S-H., Kim J-N. Reactive adsorption of sulfur compounds in diesel on nickel supported on mesoporous silica. *Appl. Catal. B Environ.*, **81**: 244–50 (2008).
  45. Samadi-Maybodi A., Teymouri M., Vahid A., Miranbeigi A. In situ incorporation of nickel nanoparticles into the mesopores of MCM-41 by manipulation of solvent–solute interaction and its activity toward adsorptive desulfurization of gas oil. *J. Hazard. Mater.*, **192**: 1667–74 (2011).
  46. Montazerolghaem M., Seyedeyn-Azad F., Rahimi A. The performance of pelletized Ce-Y and Ni-Y zeolites for removal of thiophene from model gasoline solutions. *Korean J. Chem. Eng.*, **32**: 328–34 (2015).
  47. Ko CH., Park JG., Park JC., Song H., Han S-S., Kim J-N. Surface status and size influences of nickel nanoparticles on sulfur compound adsorption. *Appl. Surf. Sci.*, **253**: 5864–5867 (2007).
  48. Ma X., Velu S., Kim JH., Song C. Deep desulfurization of gasoline by selective adsorption over solid adsorbents and impact of analytical methods on ppm-level sulfur quantification for fuel cell applications. *Appl. Catal. B Environ.*, **56**: 137–47 (2005).
  49. Moosavi E., Dastgheib S., Karimzadeh R. Adsorption of Thiophenic Compounds from Model Diesel Fuel Using Copper and Nickel Impregnated Activated Carbons. *Energies*, **5**: 4233–50 (2012).
  50. Xiong J., Zhu W., li H., Ding W., Chao Y., Wu P., Xun S., Zhang M., Li H. Few-layered graphene-like boron nitride induced a remarkable adsorption capacity for dibenzothiophene in fuels. *Green Chem.*, **17**: 1647-1656 (2014).